Title

Improved Sensitivity and Reader Confidence in CT Colonography Using Dual-Layer Spectral CT: A Phantom Study

Journal

Radiology, 297(1)

ISSN

0033-8419

Authors

Obmann, Markus M
An, Chansik
Schaefer, Amanda
et al.

Publication Date

2020-10-01

DOI

10.1148/radiol.2020200032

Peer reviewed

Radiology

ORIGINAL RESEARCH • GASTROINTESTINAL IMAGING

Improved Sensitivity and Reader Confidence in CT Colonography Using Dual-Layer Spectral CT: A Phantom Study

Markus M. Obmann, MD • Chansik An, MD • Amanda Schaefer, MD • Yuxin Sun, MS • Zhen J. Wang, MD • Judy Yee, MD • Benjamin M. Yeh, MD

From the Department of Radiology and Biomedical Imaging, University of California, San Francisco, 513 Parnassus Ave, San Francisco, CA 94117 (M.M.O., C.A., A.S., Y.S., Z.J.W., B.M.Y.); and Department of Radiology, Albert Einstein College of Medicine, Montefiore Medical Center, New York, NY (J.Y.). Received January 15, 2020; revision requested February 28; revision received May 22; accepted May 26. **Address correspondence to** B.M.Y. (e-mail: *Benjamin.Yeh@ucsf.edu*).

Supported by a grant from Philips Healthcare and the National Institute of Diabetes and Digestive and Kidney Diseases of the National Institutes of Health (R42DK104580).

Conflicts of interest are listed at the end of this article.

Radiology 2020; 297:99–107 • https://doi.org/10.1148/radiol.2020200032 • Content codes: GI CT

Background: Limited cathartic preparations for CT colonography with fecal tagging can improve patient comfort but may result in nondiagnostic examinations from poorly tagged stool. Dual-energy CT may overcome this limitation by improving the conspicuity of the contrast agent, but more data are needed.

Purpose: To investigate whether dual-energy CT improves polyp detection in CT colonography compared with conventional CT at different fecal tagging levels in vitro.

Materials and Methods: In this HIPAA-compliant study, between December 2017 and August 2019, a colon phantom 30 cm in diameter containing 60 polyps of different shapes (spherical, ellipsoid, flat) and size groups (5–9 mm, 11–15 mm) was constructed and serially filled with simulated feces tagged with four different iodine concentrations (1.26, 2.45, 4.88, and 21.00 mg of iodine per milliliter), then it was scanned with dual-energy CT with and without an outer fat ring to simulate large body size (total diameter, 42 cm). Two readers independently reviewed conventional 120-kVp CT and 40-keV monoenergetic dual-energy CT images to record the presence of polyps and confidence (three-point scale.) Generalized estimating equations were used for sensitivity comparisons between conventional CT and dual-energy CT, and a Wilcoxon signed-rank test was used for reader confidence.

Results: Dual-energy CT had higher overall sensitivity for polyp detection than conventional CT (58.8%; 95% confidence interval [CI]: 49.7%, 67.3%; 564 of 960 polyps vs 42.1%; 95% CI: 32.1%, 52.8%; 404 of 960 polyps; $P < .001$), including with the fat ring (48% and 31%, $P < .001$). Reader confidence improved with dual-energy CT compared with conventional images on all tagging levels ($P < .001$). Interrater agreement was substantial ($\kappa = 0.74$; 95% CI: 0.70, 0.77).

Conclusion: Compared with conventional 120-kVp CT, dual-energy CT improved polyp detection and reader confidence in a dedicated dual-energy CT colonography phantom, especially with suboptimal fecal tagging.

Colorectal cancer is the second most common cause of cancer death in developed countries (1). Screening for colorectal cancer, now recommended to start at age 45 years, reduces the incidence and mortality of colorectal cancer (2). Screening methods include stool-based and visual-based tests (3–5). Of the visual-based screening methods, CT colonography is less invasive and results in fewer complications than does optical colonoscopy (6). Compared with optical colonography, CT colonography has advantages: faster speed, absence of sedation, fewer complications, cost-effectiveness, and the ability to evaluate beyond obstruction or challenging anatomy (7,8). However, the colonic preparation for CT colonography remains a main reason for patient dissatisfaction and nonadherence (9). Fecal tagging and limited cathartic colon cleansing have been proposed to improve patient comfort. Fecal tagging also has the advantage of improving the detection of flat lesions (10,11).

Unfortunately, fecal tagging preparations are prone to interpatient variability and may result in inadequate fecal tagging, which can compromise confidence in the interpretation of a CT colonography scan (12). To overcome the problem of poor fecal tagging, small series and case reports suggest that dual-energy CT may improve the visualization of faint amounts of contrast material to allow for differentiation from polyps (13–17). Low-kiloelectron-volt (range, 40–60 keV) dual-energy CT virtual monoenergetic reconstructions accentuate iodine-based contrast enhancement (18,19).

For CT colonography, comparing dual-energy CT with conventional CT is challenging in actual patients. It is difficult and unethical to rescan individuals with different colonic preparations and scanning techniques before polypectomy. Furthermore, the degree of stool tagging and colonic position and distention are hard to control in vivo. In addition, it is challenging to accumulate large numbers of proven polyps of different shapes and sizes (20). Thus, a dedicated colon phantom study is needed to provide foundational data on the value of dual-energy CT versus conventional CT for polyp detection in CT colonography.

Abbreviations

CI = confidence interval, IQR = interquartile range

Summary

When compared with conventional 120-kVp CT, dual-energy CT improved the detection and reader confidence of polyps in poorly tagged CT colonography examinations.

Key Results

- Dual-energy CT had higher overall sensitivity compared with conventional CT (58.8% vs 42.1%, $P < .001$) in polyp detection.
- Reader confidence in polyp detection improved with dual-energy CT images compared with conventional images on all tagging levels ($P < .001$); interrater agreement was substantial ($\kappa = 0.74$).
- Dual-energy CT images had better sensitivity than conventional CT images for all different levels of impaired fecal tagging (all $P < .03$).

Previous CT colonography phantom studies tested only conventional CT but not dual-energy CT (21–26). For dual-energy CT, the colonic phantom must simulate human tissue and physiologic stool attenuation not only at 120 kVp but also across the different photon energies.

The aim of our study was to investigate whether low-kiloelectron-volt monoenergetic dual-energy CT improves polyp detection and reader confidence in CT colonography with impaired fecal tagging compared with conventional CT images in a phantom that mimics the spectral attenuation values of tissue, feces, and contrast at dual-energy CT.

Materials and Methods

This Health Insurance Portability and Accountability Act–compliant institutional review board–approved study was conducted between December 2017 and August 2019; the need for informed consent was waived.

Philips Healthcare provided funding as part of a research grant; they had no influence on the data for this study.

CT Colonography Phantom

An anthropomorphic colon phantom for dual-energy CT imaging was constructed. The chosen materials simulated both human tissue CT attenuation values at 120 kVp and the full energy spectrum at dual-energy CT. To simulate fat, a composite polyurethane resin (Instacast; Douglas and Sturgess, Richmond, Calif) with low-density silica (Nextrast, Burlingame, Calif) was used to cast two clamshell-design phantoms in the shape and size of a human colon. To simulate the soft tissue of the bowel wall, the lumen was coated (<3 mm) with polyurethane rubber (VytaFlex 30; Smooth-On, Macungie, Pa) doped with magnesium and tantalum oxide to obtain a constant attenuation at 50 HU across all energies (Fig 1a). The same material was used to cast polyps in three different shapes (spherical, ellipsoid, and flat), with flat lesions measuring less than 3 mm in height (27). The molds for these polyps were three-dimensionally printed in two size categories: The longest diameters were 6–9 mm (small) and 11–15 mm (big). These size groups were used to assess the effect of polyp size on detection rates.

A total of 10 polyps of each size group and shape were affixed to the walls of both colon phantoms (Fig 1b–1d). For CT scanning, the two colons were placed separately in an ellipsoid 30 × 23 cm encasement (Fig 1e) cast with the same composite resin. To simulate a larger patient size, examinations were also performed with an additional outer fat ring of adipose-equivalent plastic (CIRS, Norfolk, Va) with a 42 × 35 cm ellipsoid cross section (Fig 1f).

A stool surrogate was created by mixing polyvinyl acetate, water, sodium borate, and diatomaceous earth to simulate both the spectral attenuation curve of stool and the CT texture with air inclusions. The stool surrogate was mixed with four different concentrations of iodine (Omnipaque 350; GE Healthcare, Marlborough, Mass): 1.26, 2.45, 4.88, and 21.00 mg of iodine per milliliter to simulate trace, poorly tagged, weakly tagged, and well-tagged stool, respectively. Attenuation values for the tagged stool at 120 kVp were 50, 100, 200, and 600 HU, respectively.

CT Image Acquisition

All CT colonography examinations with iodinated fecal tagging were performed with a dual-energy CT scanner (IQon; Philips Healthcare, Cleveland, Ohio). Acquisition parameters were helical scanning mode, axial acquisition plane, collimation of 64 × 0.625 mm, tube voltage of 120 kVp, tube current of 50 mAs, pitch of 1.015, rotation time of 0.5 second, matrix of 512, field of view of 350 mm without the fat ring and 463 mm with the fat ring, and volume CT dose index of 4.5 mGy. With dual-layer spectral detector dual-energy CT, true conventional 120-kVp and dual-energy CT images were acquired simultaneously. Images were reconstructed at 1-mm section thickness and 1-mm section intervals as conventional 120-kVp and 40-keV monoenergetic images.

CT Image Reading

Two board-certified radiologists (A.S., B.M.Y.; 2 and 18 years of subspecialized experience in abdominal radiology, respectively) independently read all 12 examinations individually on axial images: They first read only conventional (120-kVp) CT images and then reread the 40-keV monoenergetic dual-energy CT images. Readers knew only that all examinations contained polyps. To reduce recollection bias, examinations were provided in multiple sessions, 2 weeks apart, starting with examinations with the lowest expected detection rates. Images were read on a picture archiving and communication system workstation that allowed readers to magnify, window, and level images freely. CT images were provided in only one orientation, with the artificial stool completely surrounding all polyps (Fig 2). For any polyps perceived by the readers (both true- and false-positive findings), the section, position, and quadrantal location of the polyp in the bowel lumen were stated and recorded by a third investigator (M.M.O.) who sat behind the readers. Readers graded their confidence on a three-point Likert scale (0, 50%–75% confidence; 1, 76%–90% confidence; 2, >90% confidence).

For analysis, the two colon phantoms were each divided into 168 segments based on haustral landmarks and quadrantal

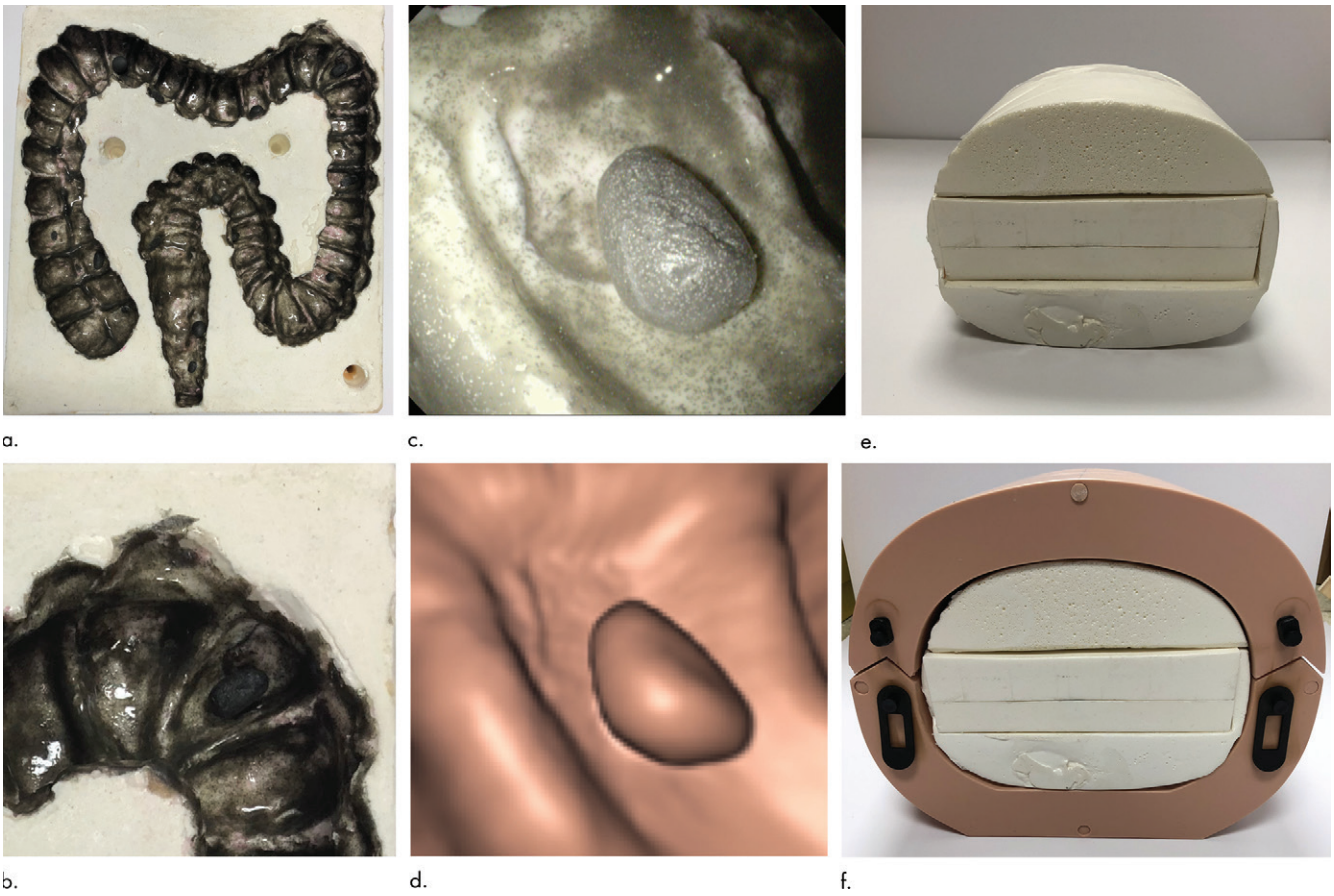

Figure 1: Colon phantom. **(a)** Half of the clam shell resin colon model. White resin simulates CT attenuation of adipose tissue, and surface of the colon lumen is coated with soft-tissue–equivalent polyurethane to simulate bowel-wall CT attenuation across the 40–200-keV x-ray spectra. **(b)** Zoomed-in view of one ellipsoid polyp in the splenic flexure of the colon phantom. **(c)** Endoscopic view of the same polyp as in **b**. **(d)** Three-dimensionally rendered image of the CT colonography scan of the same polyp as in **b**. **(e)** Fully assembled colon phantom. An anthropomorphic encasement surrounds the two halves of the colon phantom in the middle of the phantom. The diameter of the phantom is 30 cm laterally and 23 cm in the anteroposterior direction. **(f)** A fat ring of material that simulates adipose tissue across the 40–200-keV x-ray spectra is placed around the assembled phantom to increase the lateral diameter to 42 cm and the anteroposterior diameter to 35 cm.

orientation, resulting in a total of 336 colonic segments (276 segments without a polyp, 60 segments with a polyp).

Statistical Analysis

Interrater agreement was tested by using the Cohen κ statistic. Values were interpreted as proposed by Landis and Koch: a κ value of 0–0.20 indicated slight agreement; a κ value of 0.21–0.40, fair agreement; a κ value of 0.41–0.60, moderate agreement; a κ value of 0.61–0.80, substantial agreement; and a κ value of 0.81–1, almost perfect agreement (28). Sensitivities for polyps and different levels of stool tagging, polyp size, and shape were calculated. Differences were compared by using generalized estimating equation modeling with logit link function to account for clustering in the data related to the use of two phantoms, repeated scanning of these at different tagging levels, and two readers. Readers' confidence is given as the median and interquartile range (IQR), and differences between conventional and dual-energy CT images for polyps identified as true-positive findings were compared by using a Wilcoxon signed-rank test. Bonferroni correction was used for multiple comparison adjustment, and P values less than .05 were considered to indicate a significant difference. Data were analyzed by using R statistical software (version 3.2.5; R Core Team, Vienna, Austria) (29).

Results

Interrater agreement between both readers was substantial (κ = 0.74; 95% confidence interval [CI]: 0.70, 0.77).

Conventional CT had low overall sensitivity (42.1%; 95% CI: 32.1%, 52.8%; 404 of 960 polyps) for all shapes and sizes of polyps, for both readers combined, and for all scans of different tagging levels, with and without the additional fat ring. Dual-energy CT had higher sensitivity, at 58.8% (95% CI: 49.7%, 67.3%; 564 of 960 polyps; $P < .001$).

Influence of Tagging Level

Sensitivity for the different tagging levels improved with higher iodine concentration in the fecal material for both the conventional CT images (trace tagging, 11.3%; 95% CI: 7.0% 17.5%; 27 of 240) (poor tagging, 23.8%; 95% CI: 14.6% 36.3%; 57 of 240; $P = .26$ vs trace tagging) (weak tagging, 57.1%; 95% CI: 40.2%, 72.5%; 137 of 240; $P < .001$ vs trace tagging; $P = .007$ vs poor tagging) (well tagged, 76.3%; 95% CI: 68.6%, 82.5%; 198 of 240; $P < .001$ vs trace tagging; $P <$

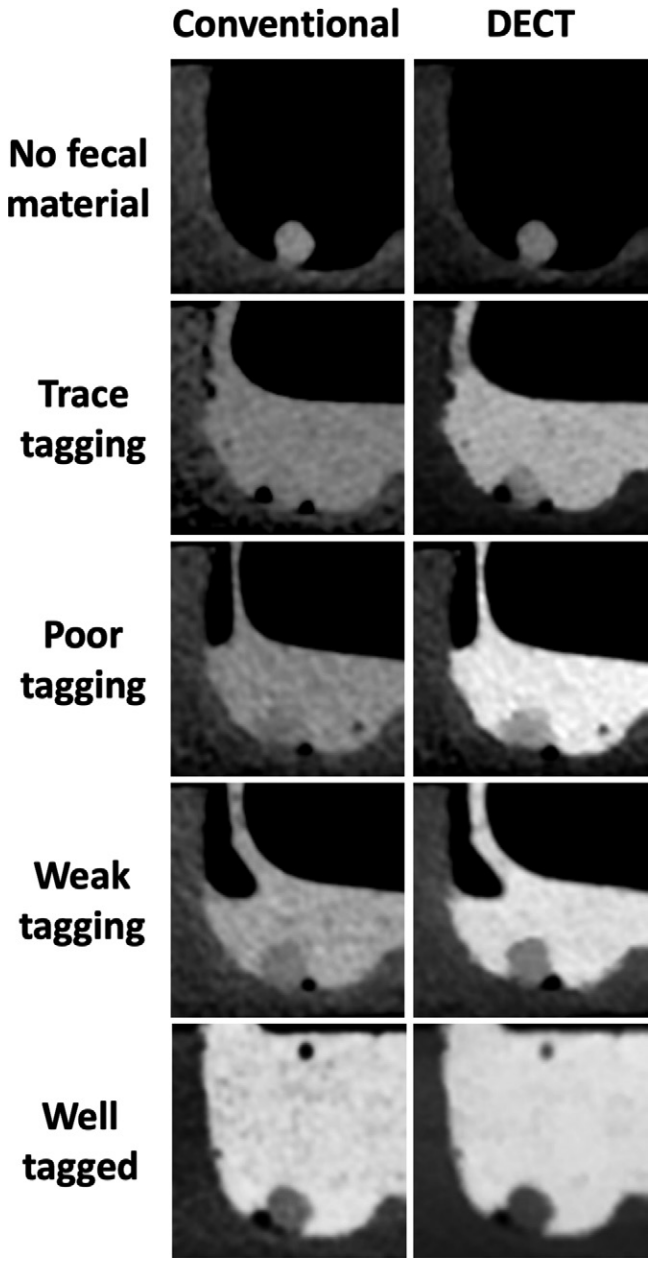

Figure 2: Examples of phantom CT scan. Conventional (left) and dual-energy 40-keV (right) scans of an ellipsoid polyp (8-mm diameter). Each column displays the polyp first with no artificial fecal material, then with increasing degrees of fecal tagging in the stool surrogate (top to bottom). DECT = dual-energy CT.

Table 1: Sensitivity and Diagnostic Performance for Polyp Detection for Different Phantom Set-ups

Scanning Set-up	Sensitivity
No fat ring	
Trace tagging	
Conventional	12.5 [7.7, 19.6] (15/120)
Spectral	32.5 [24.2, 42.1] (39/120)
P value	.03*
Poor tagging	
Conventional	38.3 [33.1, 43.9] (46/120)
Spectral	66.7 [59.0, 73.5] (80/120)
P value	<.001*
Weak tagging	
Conventional	79.2 [77.8, 80.5] (95/120)
Spectral	86.7 [82.1, 90.2] (104/120)
P value	.005*
Well tagged	
Conventional	84.2 [74.3, 90.7] (101/120)
Spectral	92.5 [77.0, 97.8] (111/120)
P value	>.99
Fat ring	
Trace tagging	
Conventional	10 [4.2, 21.9] (12/120)
Spectral	22.5 [14.5, 33.2] (27/120)
P value	.01*
Poor tagging	
Conventional	9.2 [4.5, 17.7] (11/120)
Spectral	37.5 [30.7, 44.8] (45/120)
P value	<.001*
Weak tagging	
Conventional	35.0 [22.9, 49.4] (42/120)
Spectral	55.0 [45.3, 64.4] (66/120)
P value	<.001*
Well-tagged	
Conventional	68.3 [65.4, 71.1] (82/120)
Spectral	76.7 [74.3.1, 78.9] (92/120)
P value	<.001*

Note.—Data are sensitivity, expressed as percentages, with 95% confidence intervals in brackets and absolute numbers in parentheses. Comparisons for sensitivity were done by using a generalized estimated equation; to correct for multiple comparisons, *P* values were adjusted with Bonferroni correction.

* *P* value indicates a significant difference.

.001 vs poor tagging; $P = .23$ vs weak tagging) and the dual-energy CT images (trace tagging, 27.5%; 95% CI: 20.8%, 35.4%; 66 of 240) (poor tagging, 52.1%; 95% CI: 40.9%, 63.1%; 125 of 240; $P = .002$ vs trace tagging) (weak tagging, 70.8%; 95% CI: 57.4%, 81.4%; 170 of 240; $P < .001$ vs trace tagging; $P = .16$ vs poor tagging) (well tagged, 85.6%; 95% CI: 75.9%, 90.5%; 203 of 240; $P < .001$ vs trace tagging; $P < .001$ vs poor tagging; $P = .34$ vs weak tagging). For reading of dual-energy CT images, sensitivity was higher compared with reading of conventional CT images for most individual tagging levels among scans with and those without the fat ring separately (Table 1, Fig 3). For scans with the added fat ring but the same radiation dose, the same tagging levels had lower sensitivity compared with scans without the fat ring, both for conventional and dual-energy CT images (Fig 3, Table 1).

Influence of Polyp Size

When we compared the overall sensitivity for polyp detection between the two size groups, bigger polyps (59.3%; 95% CI: 49.2%, 68.6%; 569 of 960) had higher sensitivity than small polyps (41.6%; 95% CI: 32.2%, 51.6%; 399 of 960; $P < .001$).

When all tagging levels were combined, dual-energy CT had higher sensitivity (small polyps, 49.4%; 95% CI: 39.6%, 59.2%;

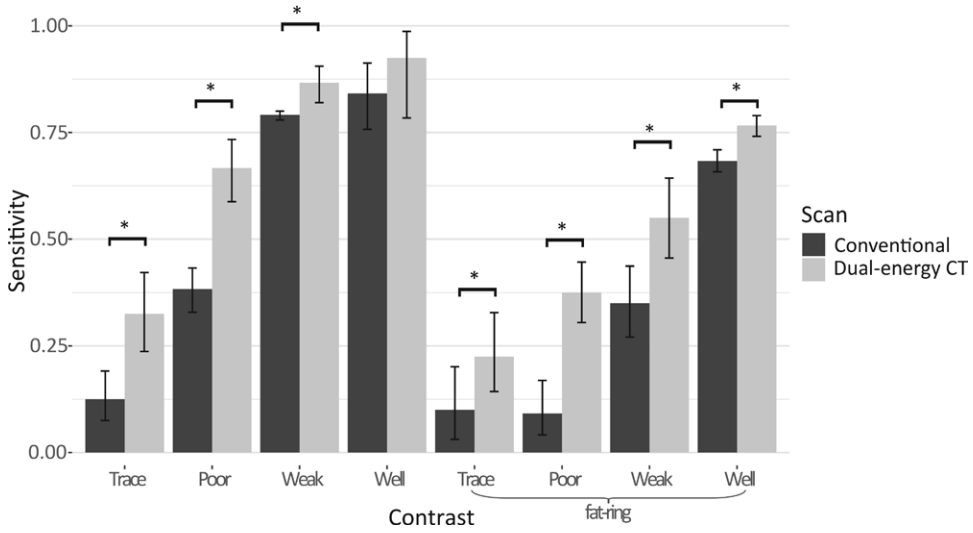

Figure 3: Overall sensitivity for polyp detection with different degrees of fecal tagging. Trace, poorly tagged, weakly tagged, and well-tagged stool corresponded to the following iodine concentrations and attenuation values on conventional (120-kVp) images: 1.26 mg of iodine per milliliter (I/mL) (50 HU), 2.45 mg I/mL (100 HU), 4.88 mg I/mL (200 HU), and 21.00 mg I/mL (600 HU), respectively. Polyps had an attenuation of 50 HU on both conventional and dual-energy CT images. Results for phantom without and within the fat ring to simulate large-body habitus are shown separately. All polyp sizes and shapes are pooled. Error bars indicate the 95% confidence interval. * Statistically significant comparisons.

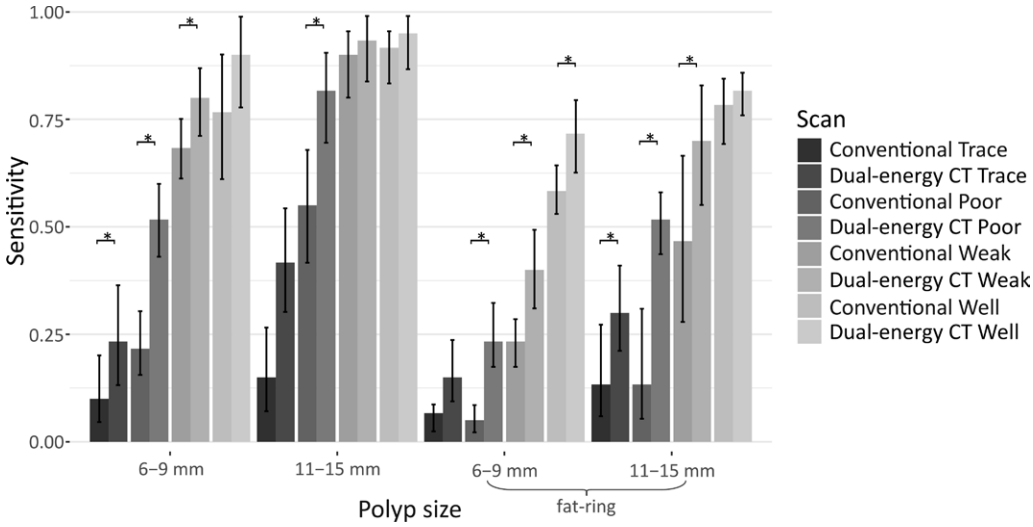

Figure 4: Sensitivity for polyp detection by polyp size. Trace, poorly tagged, weakly tagged, and well-tagged stool corresponded to the following iodine concentrations and attenuation values on conventional (120-kVp) images: 1.26 mg of iodine per milliliter (I/mL) (50 HU), 2.45 mg I/mL (100 HU), 4.88 mg I/mL (200 HU), and 21.00 mg I/mL (600 HU), respectively. Polyps had an attenuation of 50 HU on both conventional and dual-energy CT images. Results for the phantom without and within the fat ring to simulate large body habitus are shown separately. All polyp shapes are pooled. Error bars indicate the 95% confidence interval. * Statistically significant comparisons.

237 of 480) (big polyps, 68.1%; 95% CI: 59.1%, 76.0%; 327 of 480) for polyp detection than conventional CT (small polyps, 33.8%; 95% CI: 24.6%, 44.3%; 162 of 480) (big polyps, 50.4%; 95% CI: 39.0%, 61.8%; 242 of 480) in both size groups (both $P < .001$).

Subgroup analysis of small polyps of examinations with the fat ring had improved sensitivity when dual-energy CT was used compared with conventional CT for poor tagging (23.3%; 95% CI: 16.8%, 31.4%; 14 of 60 vs 5.0%; 95% CI: 2.8%, 8.7%; three of 60), weak tagging (40.0%; 95% CI: 31.2%, 49.5%; 24 of 60 vs 23.3%; 95% CI: 13.6%, 37.0%; 14 of 60), and well-tagged stool (71.6%; 95% CI: 62.5%, 79.3%; 43 of 60 vs 58.3%; 95% CI: 52.8%, 63.6%; 35 of 60; all $P < .001$). Without use of the additional fat ring, dual-energy CT improved sensitivity for trace tagging (23.3%; 95% CI: 13.6%, 37.0%; 14 of 60 vs 10%; 95% CI: 4.7%, 20.0%; six of 60; $P < .001$), poor tagging (51.7%; 95% CI: 43.2%, 60.0%; 31 of 60; vs 21.7%; 95% CI: 15.4%, 29.6%; 13 of 60; $P = .003$), and weak tagging (80%; 95% CI: 70.8%, 86.8%; 48 of 60 vs 68.3%; 95% CI: 60.8%, 75.0%; 41 of 60; $P < .001$) (Fig 4).

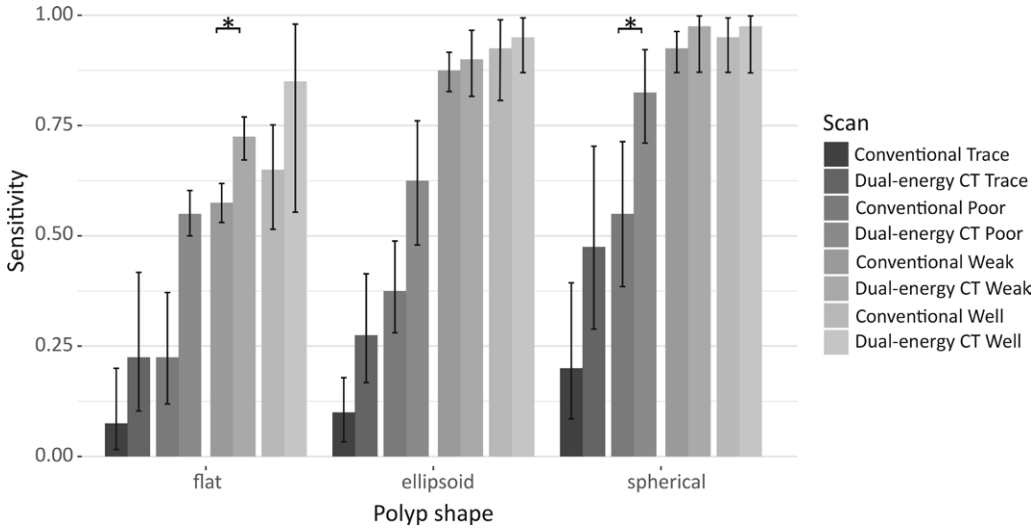

Figure 5: Sensitivity for polyp detection by polyp shape. Trace, poorly tagged, weakly tagged, and well-tagged stool corresponded to the following iodine concentrations and attenuation values on conventional (120-kVp) images: 1.26 mg of iodine per milliliter (I/mL) (50 HU), 2.45 mg I/mL (100 HU), 4.88 mg I/mL (200 HU), and 21.00 mg I/mL (600 HU), respectively. Polyps had an attenuation of 50 HU on both conventional and dual-energy CT images. Results for the phantom without the fat ring are shown. All polyp sizes are pooled. Error bars indicate the 95% confidence interval. * Statistically significant comparisons.

For large polyps, dual-energy CT improved sensitivity compared with conventional CT for examinations with the fat ring with trace tagging (30.0%; 95% CI: 21.1%, 40.6%; 18 of 60; vs 13.3%; 95% CI: 5.9%, 27.3%; eight of 60; P = .02), poor tagging (51.7%; 95% CI: 44.6%, 58.7%; 31 of 60 vs 13.3%; 95% CI: 5.1%, 30.7%; eight of 60; P = .007), and weak tagging (70.0%; 95% CI: 54.2%, 82.1%; 42 of 60; vs 46.7%; 95% CI: 28.0%, 66.3%; 28 of 60; $P < .001$). In examinations without the fat ring, sensitivity was improved only for poor tagging (81.7%; 95% CI: 73.5%, 87.8%; 49 of 60 vs 55.0%; 95% CI: 49.5%, 60.3%; 33 of 60; $P < .001$).

Influence of Polyp Shape

When we combined all tagging levels, the polyp detection sensitivity was lowest for flat lesions (34.1%; 95% CI: 25.9%, 43.3%; 218 of 640) and highest for spherical polyps (64.7%; 95% CI: 53.7%, 74.3%; 414 of 640; $P < .001$).

Dual-energy CT improved sensitivity over conventional CT for spherical polyps in examinations with poor tagging in scans without the fat ring (82.5%; 95% CI: 69.2%, 90.8%; 33 of 40 vs 55.0%; 95% CI: 38.8%, 70.2%; 22 of 40; $P < .001$) and in examinations with the fat ring with trace tagging (37.5%; 95% CI: 24.3%, 52.7%; 15 of 40 vs 17.5%; 95% CI: 8.1%, 33.9%; seven of 40), poor tagging (52.5%; 95% CI: 48.2%, 56.7%; 21 of 40 vs 10.0%; 95% CI: 10.0%, 10.0%; four of 40), and weak tagging (77.5%; 95% CI: 68.4%, 84.6%; 31 of 40 vs 57.5%; 95% CI: 44.6%, 69.5%; 23 of 40) (all $P < .001$). For ellipsoid polyps sensitivy was improved in examinations with the fat ring with poor tagging (37.5%; 95% CI: 25.8%, 50.8%; 15 of 40 vs 12.5%; 95% CI: 5.1%, 27.5%; five of 40; P = .02) and well tagged (87.5%; 95% CI: 82.6%, 91.1%; 35 of 40 vs 77.5; 95% CI: 73.0%, 81.5%; 31 of 40; $P < .001$). For flat polyps, sensitivity was only improved in examinations with weak tagging without the fat ring (72.5%; 95% CI: 68.1%, 76.5%; 29 of 40 vs 57.5%; 95% CI: 53.2%, 61.7%; 23 of 40; P = .04) (Fig 5, Table 2).

Reader Confidence

The mean overall confidence for polyp detection in correctly identified polyps was higher for dual-energy CT than for conventional CT on all tagging levels (median, 2.0 [IQR, 2.0–2.0] vs 2.0 [IQR, 1.0–2.0]; $P < .001$). Higher stool tagging levels and scans without the fat ring showed higher reader confidence. Dual-energy CT images improved reader confidence in examinations with weak tagging with the fat ring (median, 2.0 [IQR, 1.25–2.0] vs 1.0 [IQR, 1.0–2.0]; P = .04) and without the fat ring (median, 2.0 [IQR, 2.0–2.0] vs 2.0 [IQR, 1.0–2.0]; $P < .001$) and in examinations with poor tagging without the fat ring (median, 2.0 [IQR, 2.0–2.0] vs 1.0 [IQR, 1.0–2.0]; $P < .001$) (Table 3). For all false-positive polyps detected with both conventional and dual-energy CT, confidence was scored as 0.

Discussion

CT colonography is gaining importance in colorectal cancer screening. Satisfactory colonic preparation with fecal tagging remains a challenge and a major limitation. In our study, we built a spectral colon phantom to assess the additional value of dual-energy CT in polyp detection and reader confidence in cases with various levels of impaired fecal tagging to overcome this limitation. Our study showed improved sensitivity for polyp detection with reading of dual-energy CT virtual 40-keV reconstructions compared with conventional 120-kVp CT images (sensitivity, 58.8% vs 42.1%; $P < .001$). At dual-energy CT, polyp detection sensitivity improved for flat, ellipsoid, and spherical polyp shapes and for small and large polyps, as well as for different patient sizes. Furthermore, reader confidence improved with 40-keV reconstructions compared with 120-kVp images (1.77 vs 1.54, $P < .001$).

The CT colonography phantom simulated a human colon in terms of anatomic details (haustral folds) and in spectral attenuation curves both for the tissues (abdominal fat, polyp, and bowel wall attenuation) and for the tagged fecal material. We tested very low levels of fecal tagging (trace, poor, and weak tagging [range, 80–200 HU]), considered nondiagnostic in current standard imaging, and a normal level of fecal tagging (well tagged, 600 HU).

Although no prior studies of clinical or phantom scans reported on the diagnostic performance of dual-energy CT

Table 2: Subgroup Analysis of Polyp Detection Rates for Different Polyp Shapes

	Sensitivity		
Scanning Set-up	Spherical	Ellipsoid	Flat
No fat ring			
Trace tagging			
Conventional	20.0 [8.7, 39.7] (8/40)	10.0 [4.9, 19.4] (4/40)	7.5 [2.5, 20.7] (3/40)
Spectral	47.5 [27.0, 68.9] (19/40)	27.5 [16.7, 41.8] (11/40)	22.5 [11.2, 40.0] (9/40)
P value	.10	.90	>.99
Poor tagging			
Conventional	55.0 [38.8, 70.2] (22/40)	37.5 [27.6, 48.6] (15/40)	22.5 [12.3, 37.6] (9/40)
Spectral	82.5 [69.2, 90.8] (33/40)	62.5 [47.3, 75.6] (25/40)	55.0 [50.0, 59.8] (22/40)
P value	<.001*	>.99	.06
Weak tagging			
Conventional	92.5 [87.0, 95.8] (37/40)	87.5 [82.6, 91.2] (35/40)	57.5 [53.2, 61.7] (23/40)
Spectral	97.5 [87.2, 99.9] (39/40)	90.0 [80.6, 95.1] (36/40)	72.5 [68.1, 76.5] (29/40)
P value	>.99	>.99	.04*
Well tagged			
Conventional	95.0 [87.1, 98.1] 38/40	92.5 [79.3, 97.5] (37/40)	65.0 [46.1, 80.1] (26/40)
Spectral	97.5 [87.2, 99.9] (39/40)	9.50 [87.1, 98.2] (38/40)	85.0 [53.7, 96.5] (34/40)
P value	>.99	>.99	>.99
Fat ring			
Trace tagging			
Conventional	17.5 [8.1, 33.9] (7/40)	10.0 [3.6, 24.8] (4/40)	2.5 [0.4, 12.8] (1/40)
Spectral	37.5 [24.4, 52.7] (15/40)	20.0 [10.6, 34.6] (8/40)	10.0 [4.9, 19.4] (4/40)
P value	<.001*	.76	>.99
Poor tagging			
Conventional	10.0 [10.0, 10.0] (4/40)	12.5 [5.1, 27.5] (5/40)	5.0 [0.9, 23.9] (2/40)
Spectral	52.5 [48.2, 56.7] (21/40)	37.5 [25.8, 50.8] (15/40)	22.5 [15.4, 31.6] (9/40)
P value	<.001*	.02*	>.99
Weak tagging			
Conventional	57.5 [44.6, 69.5] (23/40)	32.5 [14.8, 57.1] (13/40)	15.0 [7.0, 29.4] (6/40)
Spectral	77.5 [68.3, 84.6] (31/40)	60.0 [47.6, 71.2] (24/40)	27.5 [15.5, 44.0] (11/40)
P value	<.001*	.06	<.001*
Well-tagged			
Conventional	97.5 [87.2, 99.6] (39/40)	77.5 [73.0, 81.5] (31/40)	30.0 [21.2, 40.6] (12/40)
Spectral	97.5 [87.2, 99.6] (39/40)	87.5 [82.6, 91.2] (35/40)	45.0 [34.4, 56.0] (18/40)
P value	>.99	<.001*	0.45

Note.—Data are sensitivity, expressed as percentages, with 95% confidence intervals in brackets and absolute numbers in parentheses. Comparisons for sensitivity were done by using a generalized estimated equation; to correct for multiple comparisons, *P* values were adjusted with Bonferroni correction.

* *P* value indicates a significant difference.

versus conventional CT for CT colonography, we found lower sensitivities for polyps than those reported in other clinical studies using conventional CT colonography (30). One reason for our lower sensitivity is likely our focus on low-level stool tagging, which made polyp detection challenging. In addition, we included flat lesions thinner than 3 mm, which have a lower detection rate at CT colonography. Moreover, our phantoms were viewed in only one position (prone), with all polyps being covered by artificial stool. Our low observed sensitivities may also explain why some of our subgroup analyses did not show an improvement in polyp detection rate with low-kiloelectronvolt images compared with 120-kVp images because readers detected only low numbers of polyps.

Common concerns for the clinical use of dual-energy CT include the potential need for higher radiation dose than for conventional CT and the need to preselect patients for dual-energy CT protocols versus conventional CT. With the spectral-detector–based dual-energy CT system we used, the dual-energy data set is always acquired simultaneously with the conventional (120-kVp) images without any dose penalty or the need for a separate imaging protocol. The scans we obtained are in the low-dose spectrum, with a volume CT dose index of 4.5 mGy (31). Because the volume CT dose index was the same for scans obtained with and those obtained without the fat ring, higher image noise explains the lower sensitivity for polyp detection in the larger phantom. For large patients with a body size equivalent

Table 3: Reader Confidence for Correct Polyp Detection

	No Fat Ring		Fat Ring	
Scanning Set-up	No. of Polyps Detected	Confidence	No. of Polyps	Confidence
Trace tagging	15	…	12	…
Conventional	…	1.00 (1.00–1.00)	…	1.00 (0.75–1.00)
Spectral	…	2.00 (1.00–2.00)	…	1.00 (1.00–2.00)
P value	…	.46	…	.56
Poor tagging	46		11	…
Conventional	…	1.00 (1.00–2.00)	…	1.00 (0.00–1.00)
Spectral	…	2.00 (2.00–2.00)	…	2.00 (1.00–2.00)
P value	…	<.001*	…	.09
Weak tagging	95	…	42	…
Conventional	…	2.00 (1.00–2.00)	…	1.00 (1.00–2.00)
Spectral	…	2.00 (2.00–2.00)	…	2.00 (1.25–2.00)
P value	…	<.001*	…	.04*
Well tagged	101	…	81	…
Conventional	…	2.00 (2.00–2.00)	…	2.00 (2.00–2.00)
Spectral	…	2.00 (2.00–2.00)	…	2.00 (2.00–2.00)
P value	…	>.99	…	>.99

Note.—Unless otherwise indicated, data are medians, with the interquartile range in parentheses. Comparisons were made by using Wilcoxon signed-rank test; to correct for multiple comparisons, *P* values were adjusted with Bonferroni correction.

* *P* values indicate a significant difference.

to that represented by the fat ring scans, a compensatory higher radiation dose could certainly be chosen. Nevertheless, despite the higher noise, 40-keV monoenergetic images still improved sensitivity compared with 120-kVp images for the larger simulated body size.

Our study had several limitations. First, our study was limited to phantoms, without actual patients. However, use of phantoms allowed precise polyp size and shape and fecal tagging levels without concern for interscan variation, such as degree of colonic distention or undue radiation, which would be impractical and unethical in patients. Second, because of the use of the same phantom for repeated scans, recall bias may have resulted in additionally detected polyps for both conventional and dual-energy CT; therefore, the beneficial effect of dual-energy CT may be underestimated. Third, we used only axial images for image review, without three-dimensional reformations. Because of the low levels of fecal tagging and the large amount of stool, conventional electronic cleansing of the bowel was not possible and would have resulted in the conventional image data set not being cleansed at all, without meaningful three-dimensional depiction of the submerged polyps. Fourth, our study was performed with a dual-layer spectral detector dual-energy CT system. Although virtual monoenergetic images can be generated with all dual-energy CT platforms, the anticorrelated noise suppression of dual-energy CT may provide a higher signal-to-noise ratio for low-kiloelectron-volt virtual monoenergetic images (32). Therefore, results may not transfer to other dual-energy CT platforms because 40-keV images might be less favorable for other dual-energy CT systems.

In conclusion, in a dual-energy CT colonography phantom with suboptimally tagged stool, low-kiloelectron-volt dual-energy CT improved the detection of polyps, as well as reader confidence compared with conventional 120-kVp images. Future study of dual-energy CT-augmented electronic stool subtraction, which is not currently clinically available, will be needed to assess three-dimensional evaluation. In addition, further clinical study of dual-energy CT reconstructions in CT colonography for various platforms is warranted. Such a technique may salvage cases of suboptimal fecal tagging or reduce the amount of oral contrast medium needed for bowel preparation.

Author contributions: Guarantors of integrity of entire study, M.M.O., B.M.Y.; study concepts/study design or data acquisition or data analysis/interpretation, all authors; manuscript drafting or manuscript revision for important intellectual content, all authors; approval of final version of submitted manuscript, all authors; agrees to ensure any questions related to the work are appropriately resolved, all authors; literature research, M.M.O., B.M.Y.; experimental studies, M.M.O., A.S., Y.S., J.Y., B.M.Y.; statistical analysis, M.M.O., C.A.; and manuscript editing, M.M.O., C.A., A.S., Z.J.W., J.Y., B.M.Y.

Disclosures of Conflicts of Interest: M.M.O. disclosed no relevant relationships. **C.A.** disclosed no relevant relationships. **A.S.** disclosed no relevant relationships. **Y.S.** Activities related to the present article: disclosed no relevant relationships. Activities not related to the present article: has stock in Nextrast. Other relationships: disclosed no relevant relationships. **Z.J.W.** Activities related to the present article: disclosed no relevant relationships. Activities not related to the present article: is a consultant for GE Healthcare, has stock in Nextrast. Other relationships: disclosed no relevant relationships. **J.Y.** Activities related to the present article: disclosed no relevant relationships. Activities not related to the present article: institution received a grant from GE Healthcare. Other relationships: institution issued a patent to Echopixel. **B.M.Y.** Activities related to the present article: disclosed no relevant relationships. Activities not related to the present article: is a consultant for GE Healthcare and Perspectum; has provided personal injury expert consultation for legal cases; institution received grants from Philips Healthcare, GE Healthcare, and Guerbet; gave lectures for Philips Healthcare and GE Healthcare; is the coinventor of UCSF patents licensed to Nextrast, with royalties paid to UCSF, and in turn receives part of those royalties from UCSF; receives royalties from Oxford University Press; is a major shareholder in and receives paid travel and accommodations to consult for Nextrast. Other relationships: disclosed no relevant relationships.

References

1. Siegel RL, Miller KD, Jemal A. Cancer statistics, 2018. CA Cancer J Clin 2018;68(1):7–30.
2. Wolf AMD, Fontham ETH, Church TR, et al. Colorectal cancer screening for average-risk adults: 2018 guideline update from the American Cancer Society. CA Cancer J Clin 2018;68(4):250–281.
3. Hewitson P, Glasziou P, Watson E, Towler B, Irwig L. Cochrane systematic review of colorectal cancer screening using the fecal occult blood test (hemoccult): an update. Am J Gastroenterol 2008;103(6):1541–1549.
4. US Preventive Services Task Force; Bibbins-Domingo K, Grossman DC, et al. Screening for colorectal cancer: US Preventive Services Task Force recommendation statement. JAMA 2016;315(23):2564–2575.
5. Lin JS, Piper MA, Perdue LA, et al. Screening for colorectal cancer: a systematic review for the U.S. Preventive Services Task Force [Internet]. Rockville (MD): Agency for Healthcare Research and Quality (US); 2016 Jun. Report No.: 14-05203-EF-1. http://www.ncbi.nlm.nih.gov/pubmed/27441328. Accessed August 16, 2018.
6. Nagata K, Takabayashi K, Yasuda T, et al. Adverse events during CT colonography for screening, diagnosis and preoperative staging of colorectal cancer: a Japanese national survey. Eur Radiol 2017;27(12):4970–4978.
7. van der Meulen MP, Lansdorp-Vogelaar I, Goede SL, et al. Colorectal cancer: cost-effectiveness of colonoscopy versus CT colonography screening with participation rates and costs. Radiology 2018;287(3):901–911.
8. Liedenbaum MH, de Vries AH, Gouw CIBF, et al. CT colonography with minimal bowel preparation: evaluation of tagging quality, patient acceptance and diagnostic accuracy in two iodine-based preparation schemes. Eur Radiol 2010;20(2):367–376.
9. Beebe TJ, Johnson CD, Stoner SM, Anderson KJ, Limburg PJ. Assessing attitudes toward laxative preparation in colorectal cancer screening and effects on future testing: potential receptivity to computed tomographic colonography. Mayo Clin Proc 2007;82(6):666–671.
10. Kim DH, Lubner MG, Cahoon AR, Pooler BD, Pickhardt PJ. Flat serrated polyps at CT colonography: relevance, appearance, and optimizing interpretation. RadioGraphics 2018;38(1):60–74.
11. Kim DH, Hinshaw JL, Lubner MG, Munoz del Rio A, Pooler BD, Pickhardt PJ. Contrast coating for the surface of flat polyps at CT colonography: a marker for detection. Eur Radiol 2014;24(4):940–946.
12. Yeh BM, Obmann MM, Westphalen AC, et al. Dual energy computed tomography scans of the bowel: benefits, pitfalls, and future directions. Radiol Clin North Am 2018;56(5):805–819.
13. Eliahou R, Azraq Y, Carmi R, Mahgerefteh SY, Sosna J. Dual-energy based spectral electronic cleansing in non-cathartic computed tomography colonography: an emerging novel technique. Semin Ultrasound CT MR 2010;31(4):309–314.
14. Cai W, Kim SH, Lee J-GG, Yoshida H. Virtual colon tagging for electronic cleansing in dual-energy fecal-tagging CT colonography. Eng Med Biol Soc (EMBC), 2012 Annu Int Conf IEEE. IEEE, 2012; 3736–3739. http://ieeexplore.ieee.org/abstract/document/6346779/. Accessed December 4, 2017.
15. Cai W, Lee JG, Zhang D, Kim SH, Zalis M, Yoshida H. Electronic cleansing in fecal-tagging dual-energy CT colonography based on material decomposition and virtual colon tagging. IEEE Trans Biomed Eng 2015;62(2):754–765.
16. Karcaaltincaba M, Karaosmanoglu D, Akata D, Sentürk S, Ozmen M, Alibek S. Dual energy virtual CT colonoscopy with dual source computed tomography: initial experience. Rofo 2009;181(9):859–862.
17. Carmi R, Kafri G, Goshen L, et al. A unique noncathartic CT colonography approach by using two-layer dual-energy MDCT and a special algorithmic colon cleansing method. Nucl Sci Symp Conf Rec 2008 NSS'08 IEEE. IEEE, 2008; 4780–4783. http://ieeexplore.ieee.org/abstract/document/4774312/. Accessed October 6, 2017.
18. Große Hokamp N, Höink AJ, Doerner J, et al. Assessment of arterially hyperenhancing liver lesions using virtual monoenergetic images from spectral detector CT: phantom and patient experience. Abdom Radiol (NY) 2018;43(8):2066–2074.
19. Hickethier T, Byrtus J, Hauger M, et al. Utilization of virtual mono-energetic images (MonoE) derived from a dual-layer spectral detector CT (SDCT) for the assessment of abdominal arteries in venous contrast phase scans. Eur J Radiol 2018;99:28–33.
20. Zalis ME, Barish MA, Choi JR, et al. CT colonography reporting and data system: a consensus proposal. Radiology 2005;236(1):3–9.
21. Lambert L, Lambertova A, Danes J, Grusova G. Computed tomography colonography phantom: Construction, validation and literature review. Iran J Radiol 2016;13(4):e31069.
22. Branschofsky M, Vogt C, Aurich V, Beck A, Mödder U, Cohnen M. Feasibility of ultra-low-dose multi-detector-row CT-colonography: detection of artificial endoluminal lesions in an in-vitro-model with optimization of image quality using a noise reduction filter algorithm. Eur J Med Res 2006;11(1):13–19.
23. Taylor S, Slater A, Honeyfield L, Burling D, Halligan S. CT colonography: effect of colonic distension on polyp measurement accuracy and agreement-in vitro study. Acad Radiol 2006;13(7):850–859.
24. Flicek KT, Hara AK, Silva AC, Wu Q, Peter MB, Johnson CD. Reducing the radiation dose for CT colonography using adaptive statistical iterative reconstruction: A pilot study. AJR Am J Roentgenol 2010;195(1):126–131.
25. de Vries AH, Venema HW, Florie J, Nio CY, Stoker J. Influence of tagged fecal material on detectability of colorectal polyps at CT: phantom study. AJR Am J Roentgenol 2008;191(4):1101.
26. Virmani S, Lev-Toaff A, Ciancibello L. Automatic polyp detection and measurement with computed tomographic colonography: a phantom study. Biomed Imaging Interv J 2009;5(3):e15.
27. Park SH, Lee SS, Choi EK, et al. Flat colorectal neoplasms: definition, importance, and visualization on CT colonography. AJR Am J Roentgenol 2007;188(4):953–959.
28. Landis JR, Koch GG. The measurement of observer agreement for categorical data. Biometrics 1977;33(1):159–174.
29. R Core Team. R: A Language and Environment for Statistical Computing. Vienna, Austria: R Foundation for Statistical Computing, 2018. https://www.r-project.org/. Accessed January 31, 2019.
30. Fletcher JG, Chen MH, Herman BA, et al. Can radiologist training and testing ensure high performance in CT colonography? Lessons From the National CT Colonography Trial. AJR Am J Roentgenol 2010;195(1):117–125.
31. Chang KJ, Yee J. Low-dose computed tomography colonography technique. Radiol Clin North Am 2018;56(5):709–717.
32. Kalender WA, Klotz E, Kostaridou L. An algorithm for noise suppression in dual energy CT material density images. IEEE Trans Med Imaging 1988;7(3):218–224.